iMRI 2022;26;256-264
https://doi.org/10.13104/imri.2022.26.4.256
pISSN 2384-1095 eISSN 2384-1109

Review Article

Received: October 13, 2022
Revised: December 2, 2022
Accepted: December 9, 2022

Correspondence
Mina Park, MD, PhD
Department of Radiology,
Gangnam Severance Hospital,
Yonsei University
College of Medicine,
211 Eonju-ro 63-gil, Gangnam-gu,
Seoul 06273, Korea.
E-mail: to.minapark@yuhs.ac

Dynamic Contrast-Enhanced MRI and Its Applications in Various Central Nervous System Diseases

Kuk Jin Kim, Mina Park, Bio Joo, Sung Jun Ahn, and Sang Hyun Suh

Department of Radiology, Gangnam Severance Hospital, Yonsei University College of Medicine, Seoul, Korea

Dynamic contrast-enhanced MRI (DCE-MRI) is a noninvasive imaging technique used to evaluate tissue vascularity/permeability features through consecutive imaging acquisitions after gadolinium-based contrast agent administration. Over the past several decades, techniques and protocols for DCE-MRI have evolved, leading to growing applications of DCE-MRI for different neurological disorders. Although most established applications of DCE-MRI are for studying tumors, an increasing number of studies have been evaluating the use of this technique for neurodegenerative and other miscellaneous diseases. The purpose of this article was to provide an overview of DCE-MRI and its clinical applications in various neurological diseases.

Keywords: Brain; Magnetic resonance imaging; Central nervous system; Brain neoplasms; Neurodegenerative diseases

INTRODUCTION

A growing number of neurological conditions have been found to be related to impaired integrity of the blood-brain barrier (BBB) [1]. To investigate the role of the BBB in these diseases, in vivo methods that can measure BBB disruption, even if it is very subtle, are required. Dynamic contrast-enhanced MRI (DCE-MRI) is a noninvasive imaging technique that can be used to elucidate BBB permeability/vascularity features through consecutive imaging acquisitions after administering a gadolinium-based contrast agent (GBCA) [2]. Over the past several decades, techniques and protocols of DCE-MRI have evolved, leading to its growing applications for different neurological disorders. Although most established applications of DCE-MRI are for studying tumors, an increasing number of studies have been evaluating the use of DCE-MRI for neurodegenerative and other miscellaneous diseases. The purpose of this article was to provide an overview of DCE-MRI and its clinical applications in various neurological diseases. Before elaborating on DCE-MRI, we will briefly discuss the anatomy and role of the BBB in the central nervous system (CNS).

BBB

The BBB is a selectively permeable border of endothelial cells that can prevent solutes in the circulating blood from crossing into the extracellular fluid of the CNS [3]. The BBB functions as both a barrier and an interface between the vasculature and brain parenchyma. By regulating molecular transportation from capillaries into neuronal tissues and vice versa, the BBB maintains homeostasis of the CNS [4]. The BBB consists of endothelial cells that line the capillaries. Endothelial cells are connected by tight junctions and pericytes that wrap around endothelial cells with astrocytic end feet encircling them (Fig. 1) [5]. In many neurological disorders, a disruption of the BBB integrity plays an important role in the pathogenesis or outcome of the disease [1]. Therefore, it is crucial to evaluate BBB integrity using MRI to elucidate the role of BBB disruption in the disease. As disruption of the BBB causes extravasation of GBCAs into the extravascular extracellular space (EES), accumulated GBCAs in the EES of the disrupted brain regions can result in shortening of T1 relaxation time and finally high T1-weighted signal intensity. Using DCE-MRI, this T1 enhancement can be measured and reflected in regions showing BBB disruption [2].

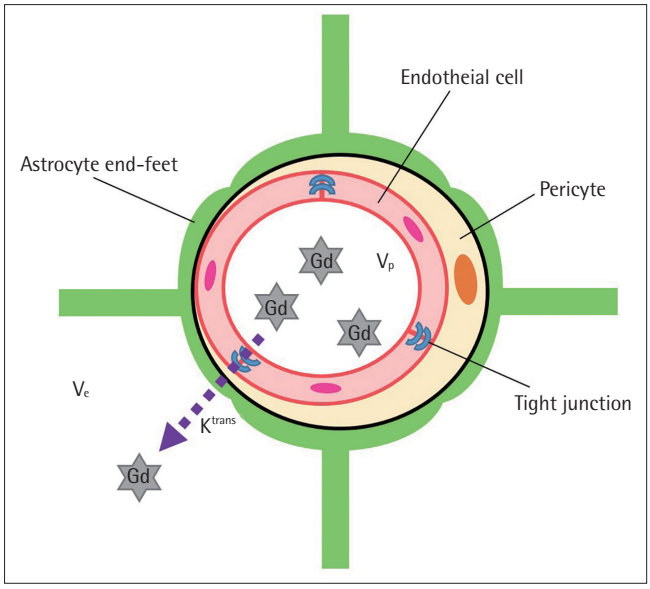

Fig. 1. Schematic figure showing the neurovascular unit and blood-brain barrier. Leakage of gadolinium (Gd)-based contrast agent across the disrupted blood-brain barrier from the capillary blood plasma space (V_p) to the extravascular extracellular space (V_e) and the permeability surface area product per unit volume of tissue (K^{trans}) are exhibited.

DCE-MRI

DCE-MRI can be obtained from repeated T1-weighted imaging acquisitions after intravenous injection of GBCAs, providing measurements of signal enhancement of the tissue as a function of time [2]. After the bolus of a GBCA is injected, hemodynamic signals of DCE-MRI depend on T1 relaxation time, as gadolinium contrast agents cause paramagnetic effects, leading to a T1 shortening effect [6]. Thus, the T1 signal intensity increases proportional to the concentration of the contrast agent in the brain tissue (Fig. 2) [6]. Considering their sizes and structure, GBCAs cannot pass an intact BBB of a healthy brain. However, when there is the disruption of the BBB, degraded tight junctions enable GBCAs to extravasate into the extravascular extracellular space through the disrupted BBB. Finally, accumulated GBCAs in the extravascular extracellular space can lead to increased T1-weighted signal intensity [7]. Combining tissue perfusion and permeability of capillaries using pharmacokinetic computations, BBB permeability can be determined. Details of the analysis are described below.

DCE-MRI Data Analysis

Signal changes on a dynamic acquisition of T1-weighted images can be assessed either by analyzing signal intensity changes (semiquantitative) or by quantifying changes in contrast medium concentrations using a pharmacokinetic modeling technique. In this review, we will focus on quantitative

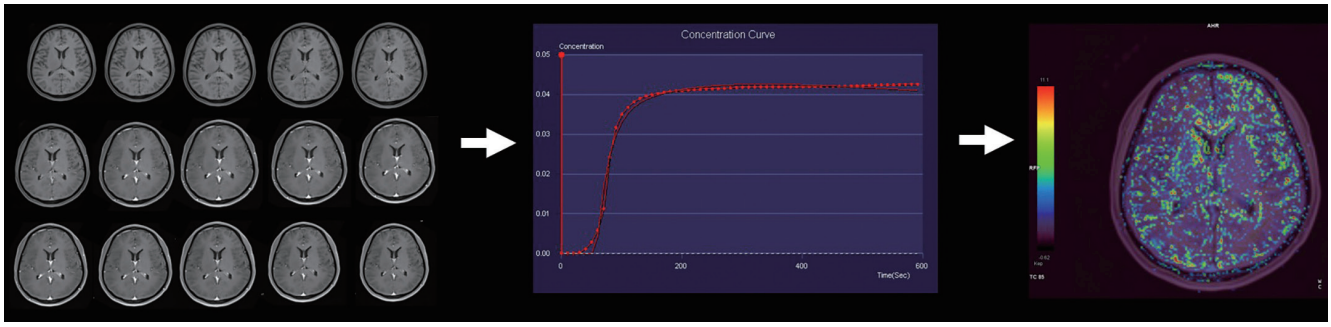

Fig. 2. Illustration of dynamic contrast-enhanced MRI in a patient. The repeated T1-weighted imaging acquisition after gadolinium-based contrast agent enables calculation of the dynamic signal enhancement and finally quantitative pharmacokinetic parameters.

pharmacokinetic modeling techniques widely used in the research field of neuroradiology.

Quantitative pharmacokinetic model-based approaches aim to offer kinetic measures with a direct relationship to tissue properties. They are simpler to interpret and less sensitive to the acquisition protocol than semiquantitative analyses [8]. Toft and colleague [9,10] first introduced a pharmacokinetic model-based analysis for DCE-MRI to calculate permeability of the BBB through a mathematical model. To describe and analyze the distribution of GBCAs, classical pharmacokinetic models generally use linear compartmental models. A compartment is defined as a distinguishable tracer distribution space. In this space, the contrast agent spreads freely [11]. However, the transport between adjacent compartments is somewhat hindered, resulting in different time concentration courses of GBCAs in each compartment [11].

There are three commonly used pharmacokinetic models: a two-compartment model, an extended Toft model, and the Patlak model (Fig. 3) [8]. The most commonly used model is the extended Toft model [9], which describes a highly perfused two-compartment tissue, considers bidirectional transport between blood plasma and the EES, and offers four principle parameters: volume transfer constant, K^{trans} (min^{-1}); volume of EES fractional volume, V_e ($0 < V_e < 1$); flux rate constant between EES and plasma, k_{ep} (min^{-1}); and fractional plasma volume, V_p (Table 1) [8,9]. The K^{trans} and the EES relate to the fundamental physiology, whereas the rate constant is the ratio of the transfer constant to the EES [12]:

$$k_{ep} = K^{trans}/V_e.$$

Under flow-limited conditions, K^{trans} equals blood plasma flow per unit volume of tissue. Under permeability-limited conditions, K^{trans} equals permeability surface area product per unit volume of tissue. Therefore, if assumptions of the model are met (i.e., the flow is high enough and the rate of contrast extravasation is low enough to ensure equal concentrations in the arteries and capillary bed), then $K^{trans} \approx$ permeability surface is a good assumption. Therefore, K^{trans} can indicate the permeability in most neuroimaging studies [13]. The extended Toft model enables us to calculate the fractional plasma volume V_p and separates enhancement effects from contrast leakage from those from intravascular contrast [8].

The Patlak model can be considered a special case of the extended Tofts model that ignores back-flux from the EES into the blood plasma compartment. Consequently, it only allows for estimation of two parameters K^{trans} and V_p [8]. V_p represents the capillary blood plasma volume fraction in a tissue. The Patlak model is now widely recommended for measuring slow leakage of the BBB in small vessel disease or neurodegenerative disease because back-flux from the EES to the capillaries is negligible in subtly leaking tissues [14].

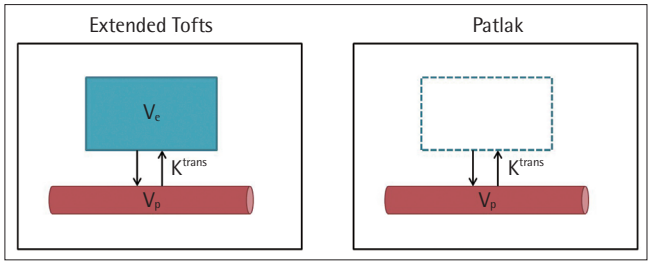

Fig. 3. Schematic illustrations of extended Toft model, Patlak model, and parameters.

Table 1. Quantitative Parameters of Dynamic Contrast-Enhanced MRI

Parameters	Represents	Unit
K^{trans}	Volume transfer constant (or coefficient) between blood plasma and extravascular extracellular space (EES) ≒ permeability surface area product (non-flow-limited situation) ≒ cerebral blood flow (flow-limited situation)	min^{-1}
V_e	Volume of EES per unit volume of tissue, $0 < V_e < 1$	None
k_{ep}	Rate constant between EES and blood plasma Reflux rate	min^{-1}
V_p	Fractional plasma volume	None

It is essential to consider the appropriateness of pharmacokinetic models in relation to a particular condition and acquisition protocols pertaining to the study. For example, the assumption of high tissue perfusion might be inappropriate for modeling rapid concentration changes that occur around the time of the first pass after a bolus injection—this might be corrected by excluding early data points from the fitting [8,15]. In this context, K^{trans} measurements in acute ischemic conditions could also be confounded by low tissue perfusion. Further assumption of negligible back-flux across the BBB might also be invalid for relatively high leakage rates sometimes found in stroke or tumor lesions [14].

DCE-MRI APPLICATIONS IN NEUROLOGICAL DISEASES

Recently, there have been a growing number of DCE-MRI studies investigating BBB integrity and its association with diseases [1]. In this review paper, we will review applications

of DCE-MRI for investigation of pathogenesis, diagnosis, and prediction of disease prognosis in neurological diseases.

Brain Tumors

DCE-MRI applications in brain tumors have been widely investigated in the literature. DCE-MRI is mainly applied to gliomas for accurate diagnosis, evaluation of treatment response, and prediction of progression. The presence of enhancement in brain tumors is considered to be due to increased vascular permeability as a result of BBB breakdown in contrast to non-enhancing tumors. Through DCE-MRI applications, we can widen this concept to quantifiable DCE-MRI-derived parameters.

It is largely accepted that higher grade glioma shows higher K^{trans}, V_e, and V_p values than lower grade glioma. Among various DCE parameters, K^{trans} is considered the most useful imaging biomarker for grading gliomas [16-20]. In glioblastoma, the BBB is partially destroyed in preexisting vessels and the BBB in angiogenic vessels forms imperfectly. Therefore, contrast leakage might be increased in poorly integrated vessels [21]. The recently introduced World Health Organization (WHO) classification of brain tumors includes molecular diagnostic criteria as well as traditional histopathologic features [22]. Increased K^{trans} and V_p values were observed in epidermal growth factor variant III (EGFRvIII)-positive glioblastoma [17]. Ahn et al. [23] have also found that glioblastomas with O^6-methylguanine-DNA methyltransferase (MGMT) methylation have higher K^{trans} values than those without methylation [23]. The same group also found that K^{trans} values were lower in lower grade gliomas with MGMT methylation than in those without methylation, suggesting that DCE-MRI might also be associated with molecular markers [24].

DCE-MRI can be also applied in tumor differential diagnosis. An atypical presentation of primary CNS lymphoma might be indistinguishable from glioblastoma on conventional brain MRI. As lymphoma exhibits a distinctive difference in vascular permeability compared with glioblastoma, T1-dominant leakage and thereby higher K^{trans} and k_{ep} values were observed in lymphoma than in glioblastoma [25,26]. Furthermore, pretreatment V_p and K^{trans} values might be prognostic biomarkers of progression in patients with lymphoma [27]. K^{trans} parameters were also found to predict treatment response in patients with lymphoma [28]. In terms of differential diagnosis of glioblastoma and metastasis, another challenging task for radiologists is that there are no significant differences between glioblastoma and metastases of different origins. However, hypovascular metastasis could be differentiated using V_p value, area under the curve, and logarithmic slope of the wash-out phase of DCE-MRI [29]. Another study has also confirmed that there is no difference between glioma and metastasis in terms of the K^{trans} value, although higher K^{trans} values of peritumoral edema area are found in glioma than in metastasis [30].

A meta-analysis has demonstrated that DCE-MRI has higher diagnostic accuracy than diffusion-weighted MRI and perfusion MRI in differentiating between treatment-induced changes and progression [31]. Increased K^{trans} values have been reported in recurrent enhancing lesions compared with radionecrosis, which may help differentiate a tumor from radionecrosis [32,33]. In patients with glioblastoma, DCE-MRI may be also applied to differentiate progression from pseudoprogression. It is known that K^{trans}, V_e, and V_p values are higher in progression than in pseudoprogression [34-36]. Recently, a radiomics analysis of DCE-MRI has shown that features obtained from K^{trans} can achieve a good accuracy in detecting pseudoprogression [37]. In particular, in patients with glioblastoma treated with bevacizumab, a higher mean k_{ep} was associated with shorter progression-free survival (PFS) and overall survival, suggesting that pretreatment mean k_{ep} might be a useful value for predicting response to bevacizumab treatment [38].

DCE-MRI in brain tumors might have an added prognostic value compared with that in gliomas. Higher K^{trans} and V_e or V_p values are also associated with a worse prognosis in patients with glioblastoma [39,40]. Kim et al. [41] have also found higher mean V_e values in patients with anaplastic astrocytoma with a shorter PFS (<18 months) than in those with a longer PFS. A radiomics approach with DCE-MRI has also been shown to be useful for predicting the prognosis of patients with glioblastoma as a radiomics risk score from DCE-MRI has been found to be associated with PFS [42].

Neurodegenerative Disease

Cerebral Small Vessel Disease

Cerebral small vessel disease (cSVD) covers a wide array of pathologies involving dysfunction of small vessels of the brain. White matter hyperintensities (WMHs) are a common finding in the elderly population and a major feature of cSVD [43,44]. While their pathogenesis remains unclear, BBB leakage is the most accepted hypothesis regarding the origin of WMH [14].

Li et al. [45] have assessed BBB permeability in patients with a low, medium, or high burden of cSVD. They found that global BBB permeability was associated with a higher WMH burden. Another study by Wardlaw et al. [46] also found a relationship between BBB permeability and WMH burden in patients with cSVD. The authors found that the healthy white matter surrounding WMHs showed increased BBB permeability, suggesting that BBB disruption might precede later extensions of WMH lesions. Moreover, a study with both dynamic susceptibility contrast MRI and DCE-MRI in patients

with cSVD has shown a negative correlation between cerebral blood flow (CBF) and BBB leakage in perilesional zones of WMH lesions, suggesting that both BBB and CBF are regulated in the neurovascular unit and that this negative correlation might be due to physiologic regulation of the neurovascular unit [47].

Alzheimer's Disease

Vascular contribution to pathophysiology of Alzheimer's disease has been increasingly recognized. As such, BBB breakdown is now considered an important factor in the development and progression of Alzheimer's disease [48].

Montagne et al. [49] first reported their findings of increased BBB permeability in the hippocampus of patients with mild cognitive impairment (MCI) compared with normal controls. A further follow-up study also confirmed locally increased BBB permeability in patients with MCI [50]. Interestingly, this study exhibited BBB permeability of the medial temporal lobe as an independent early imaging biomarker of cognitive impairment unrelated to β amyloid or tau pathology [50]. In a DCE-MRI study of early Alzheimer's disease, global BBB leakage found in patients with early Alzheimer's disease was associated with cognitive decline [51]. In a follow-up study, the group also observed a global decrease in CBF in the gray matter of patients with early Alzheimer's disease, which was correlated with increased BBB leakage [52]. APOE4, the strongest risk factor gene for Alzheimer's disease, has also been suggested to be related to increased BBB permeability in both patients with MCI and cognitively normal controls, supporting that the involvement of BBB dysfunction occurs early in the course of Alzheimer's disease [53,54].

Other Neurodegenerative Diseases

Various neurodegenerative disorders share pathological alterations of the vessel wall, resulting in BBB disruption which may initiate multiple pathways of neurodegeneration [55]. A DCE-MRI study has found increased BBB leakage in the substantia nigra and posterior white matter regions of patients with Parkinson's disease compared with healthy controls [56]. In patients with Huntington's disease, positive correlations of increased BBB permeability in the caudate nucleus with increases of disease burden score and gray matter cerebral blood volume have been demonstrated [57]. DCE-MRI studies in patients with multiple sclerosis (MS) have similarly established the presence of increased BBB leakage in white matter in MS, particularly in active MS lesions [58-60].

Stroke

There are not many studies using DCE-MRI in the field of stroke. As expected, acute ischemic stroke lesions showed higher K^{trans} values than contralateral normal tissues. These values were further increased at follow-up, suggesting increased BBB permeability along the disease course [61]. Hemorrhagic transformation, a major complication of reperfusion therapy, might be also predicted by increased BBB permeability assessed by DCE-MRI as oxidative stress due to ischemic stroke can cause BBB disruption [62]. Furthermore, permeability changes observed from kinetic curves might also predict future development of new stroke in patients with transient ischemic attacks [63].

Miscellaneous Diseases

DCE-MRI has been applied to the assessment of BBB dysfunction in many other neurological diseases such as traumatic brain injury, migraine, and reversible vasoconstriction syndrome as BBB disruption has received increased attention as one of the major pathophysiological causes of many different diseases [64-66]. A recent study has found increased K^{trans} but decreased V_p values following traumatic brain injury in vulnerable areas, including the brain cortex and cerebellum [64]. Kim et al. [65] have found that patients with migraines tend to have lower V_p values in the amygdala in association with heightened permeability in the BBB, as depicted on DCE-MRI [65]. In patients with reversible vasoconstriction syndrome, microscopic brain permeability is also increased during acute stages, although macroscopic BBB disruption is not found [66]. Dynamic changes in BBB permeability might be related to impaired cerebral microvascular compliance of reversible vasoconstriction syndrome.

LIMITATIONS

There are some limitations in using DCE-MRI. First, in cases of low leakage status, the detection of BBB leakages by DCE-MRI is difficult compared to that of large BBB leakages seen in brain tumors, acute ischemic stroke, and large arterial infracts [14,67]. Thus, when using the Patlak model, there are risks for underestimated results [68]. K^{trans} can also be overestimated especially in areas with large blood vessels, which can be a problem when analyzing the whole brain as well as interesting areas [69]. In addition, the ideal acquisition time for fine BBB permeability measurement is at least 10 to 15 minutes. Such a long time of measurement is practically impossible in the clinical field [8,14,68]. There is a reproducibility issue when applying DCE parameters directly to clinical practice as consensuses for imaging instrumentation, setup procedures, imaging technique, contrast injection protocol, modeling techniques, and arterial input function are lacking [70-74]. Furthermore, previous researches have reported significant

errors in calculated DCE-MRI pharmacokinetic parameters among different perfusion analysis software packages, resulting in poor inter-software reproducibility [70,75,76]. If these problems are not properly evaluated, the reliability of DCE-MRI results will inevitably be low. To solve this problem, DCE-MRI data for a larger number of participants in multi-centers are needed. Further research should be conducted with more data accumulated to build standardized multivendor protocols.

CONCLUSIONS AND FUTURE DIRECTIONS

A growing number of clinical studies have been published. They suggest the possibility of DCE-MRI acquisition and quantification of BBB integrity for research into the pathophysiology, diagnosis, and evaluation of treatment responses of brain tumors and neurodegenerative diseases. However, even with a large number of DCE-MRI studies, assessment of BBB disruption is mostly applied in research settings. It has not been applied in routine clinical practice yet. To overcome these issues, standardized MRI protocols are needed for image acquisition as well as for data analysis to compare studies with large study populations over various sites. In conclusion, DCE-MRI is the imaging method that is the most widely used to measure BBB integrity. Through standardization with large clinical studies, its roles might be expanded not only in the research field, but also in the real world in the near future.

Availability of Data and Material

Data sharing does not apply to this article as no datasets were generated or analyzed during the current study.

Conflicts of Interest

The authors have no potential conflicts of interest to disclose.

Author Contributions

Conceptualization: Mina Park. Funding acquisition: Mina Park. Investigation: Kuk Jin Kim, Mina Park. Methodology: Kuk Jin Kim, Mina Park. Project administration: Sung Jun Ahn, Sang Hyun Suh. Resources: Kuk Jin Kim, Mina Park. Supervision: Sang Hyun Suh. Writing—original draft: Kuk Jin Kim, Mina Park. Writing—review & editing: Bio Joo, Sung Jun Ahn, Sang Hyun Suh. Approval of final manuscript: all authors.

ORCID iDs

Kuk Jin Kim	https://orcid.org/0000-0003-2312-9520
Mina Park	https://orcid.org/0000-0002-2005-7560
Bio Joo	https://orcid.org/0000-0001-7460-1421
Sung Jun Ahn	https://orcid.org/0000-0003-0075-2432
Sang Hyun Suh	https://orcid.org/0000-0002-7098-4901

Funding Statement

This work was supported by a National Research Foundation of Korea (NRF) grant funded by the Korean government (MSIT) (No. NRF-2020R1C1C1005724).

REFERENCES

1. Sweeney MD, Zhao Z, Montagne A, Nelson AR, Zlokovic BV. Blood-brain barrier: from physiology to disease and back. Physiol Rev 2019;99:21-78.
2. Elschot EP, Backes WH, Postma AA, et al. A comprehensive view on MRI techniques for imaging blood-brain barrier integrity. Invest Radiol 2021;56:10-19.
3. Daneman R, Prat A. The blood-brain barrier. Cold Spring Harb Perspect Biol 2015;7:a020412.
4. Abbott NJ, Rönnbäck L, Hansson E. Astrocyte-endothelial interactions at the blood-brain barrier. Nat Rev Neurosci 2006;7:41-53.
5. Abbott NJ, Patabendige AA, Dolman DE, Yusof SR, Begley DJ. Structure and function of the blood-brain barrier. Neurobiol Dis 2010;37:13-25.
6. Erlemann R, Reiser MF, Peters PE, et al. Musculoskeletal neoplasms: static and dynamic Gd-DTPA--enhanced MR imaging. Radiology 1989;171:767-773.
7. Chagnot A, Barnes SR, Montagne A. Magnetic resonance imaging of blood-brain barrier permeability in dementia. Neuroscience 2021;474:14-29.
8. Heye AK, Thrippleton MJ, Armitage PA, et al. Tracer kinetic modelling for DCE-MRI quantification of subtle blood-brain barrier permeability. Neuroimage 2016;125:446-455.
9. Tofts PS, Brix G, Buckley DL, et al. Estimating kinetic parameters from dynamic contrast-enhanced T(1)-weighted MRI of a diffusable tracer: standardized quantities and symbols. J Magn Reson Imaging 1999;10:223-232.
10. Tofts PS, Kermode AG. Measurement of the blood-brain barrier permeability and leakage space using dynamic MR imaging. 1. Fundamental concepts. Magn Reson Med 1991;17:357-367.
11. Gordon Y, Partovi S, Müller-Eschner M, et al. Dynamic contrast-enhanced magnetic resonance imaging: fundamentals and application to the evaluation of the peripheral perfusion. Cardiovasc Diagn Ther 2014;4:147-164.
12. Mitchell DG. MR imaging contrast agents--what's in a name? J Magn Reson Imaging 1997;7:1-4.
13. Sourbron SP, Buckley DL. Classic models for dynamic contrast-enhanced MRI. NMR Biomed 2013;26:1004-1027.
14. Thrippleton MJ, Backes WH, Sourbron S, et al. Quantifying blood-brain barrier leakage in small vessel disease: review and consensus recommendations. Alzheimers Dement 2019;15:840-858.
15. Larsson HB, Courivaud F, Rostrup E, Hansen AE. Measurement of brain perfusion, blood volume, and blood-brain barrier permeability, using dynamic contrast-enhanced T(1)-weighted MRI at 3 tesla. Magn Reson Med 2009;62:1270-1281.

16. Choi HS, Kim AH, Ahn SS, Shin NY, Kim J, Lee SK. Glioma grading capability: comparisons among parameters from dynamic contrast-enhanced MRI and ADC value on DWI. Korean J Radiol 2013;14:487-492.
17. Arevalo-Perez J, Peck KK, Young RJ, Holodny AI, Karimi S, Lyo JK. Dynamic contrast-enhanced perfusion MRI and diffusion-weighted imaging in grading of gliomas. J Neuroimaging 2015;25:792-798.
18. Santarosa C, Castellano A, Conte GM, et al. Dynamic contrast-enhanced and dynamic susceptibility contrast perfusion MR imaging for glioma grading: preliminary comparison of vessel compartment and permeability parameters using hotspot and histogram analysis. Eur J Radiol 2016;85:1147-1156.
19. Jung SC, Yeom JA, Kim JH, et al. Glioma: application of histogram analysis of pharmacokinetic parameters from T1-weighted dynamic contrast-enhanced MR imaging to tumor grading. AJNR Am J Neuroradiol 2014;35:1103-1110.
20. Zhang N, Zhang L, Qiu B, Meng L, Wang X, Hou BL. Correlation of volume transfer coefficient Ktrans with histopathologic grades of gliomas. J Magn Reson Imaging 2012;36:355-363.
21. Cha S, Yang L, Johnson G, et al. Comparison of microvascular permeability measurements, K(trans), determined with conventional steady-state T1-weighted and first-pass T2*-weighted MR imaging methods in gliomas and meningiomas. AJNR Am J Neuroradiol 2006;27:409-417.
22. Louis DN, Perry A, Wesseling P, et al. The 2021 WHO classification of tumors of the central nervous system: a summary. Neuro Oncol 2021;23:1231-1251.
23. Ahn SS, Shin NY, Chang JH, et al. Prediction of methylguanine methyltransferase promoter methylation in glioblastoma using dynamic contrast-enhanced magnetic resonance and diffusion tensor imaging. J Neurosurg 2014;121:367-373.
24. Ahn SH, Ahn SS, Park YW, Park CJ, Lee SK. Association of dynamic susceptibility contrast- and dynamic contrast-enhanced magnetic resonance imaging parameters with molecular marker status in lower-grade gliomas: a retrospective study. Neuroradiol J 2022 May 9. [Epub]. Available from: http://doi.org/10.1177/19714009221098369.
25. Kickingereder P, Sahm F, Wiestler B, et al. Evaluation of microvascular permeability with dynamic contrast-enhanced MRI for the differentiation of primary CNS lymphoma and glioblastoma: radiologic-pathologic correlation. AJNR Am J Neuroradiol 2014;35:1503-1508.
26. Zhang HW, Lyu GW, He WJ, et al. Differential diagnosis of central lymphoma and high-grade glioma: dynamic contrast-enhanced histogram. Acta Radiol 2020;61:1221-1227.
27. Hatzoglou V, Oh JH, Buck O, et al. Pretreatment dynamic contrast-enhanced MRI biomarkers correlate with progression-free survival in primary central nervous system lymphoma. J Neurooncol 2018;140:351-358.
28. Fu F, Sun X, Li Y, et al. Dynamic contrast-enhanced magnetic resonance imaging biomarkers predict chemotherapeutic responses and survival in primary central-nervous-system lymphoma. Eur Radiol 2021;31:1863-1871.
29. Jung BC, Arevalo-Perez J, Lyo JK, et al. Comparison of glioblastomas and brain metastases using dynamic contrast-enhanced perfusion MRI. J Neuroimaging 2016;26:240-246.
30. Shi Z, Jiang J, Xie L, Zhao X. Efficacy evaluation of contrast-enhanced magnetic resonance imaging in differentiating glioma from metastatic tumor of the brain and exploration of its association with patients' neurological function. Front Behav Neurosci 2022;16:957795.
31. van Dijken BRJ, van Laar PJ, Holtman GA, van der Hoorn A. Diagnostic accuracy of magnetic resonance imaging techniques for treatment response evaluation in patients with high-grade glioma, a systematic review and meta-analysis. Eur Radiol 2017;27:4129-4144.
32. Morabito R, Alafaci C, Pergolizzi S, et al. DCE and DSC perfusion MRI diagnostic accuracy in the follow-up of primary and metastatic intra-axial brain tumors treated by radiosurgery with cyberknife. Radiat Oncol 2019;14:65.
33. Bisdas S, Naegele T, Ritz R, et al. Distinguishing recurrent high-grade gliomas from radiation injury: a pilot study using dynamic contrast-enhanced MR imaging. Acad Radiol 2011;18:575-583.
34. Yun TJ, Park CK, Kim TM, et al. Glioblastoma treated with concurrent radiation therapy and temozolomide chemotherapy: differentiation of true progression from pseudoprogression with quantitative dynamic contrast-enhanced MR imaging. Radiology 2015;274:830-840.
35. Thomas AA, Arevalo-Perez J, Kaley T, et al. Dynamic contrast enhanced T1 MRI perfusion differentiates pseudoprogression from recurrent glioblastoma. J Neurooncol 2015;125:183-190.
36. Suh CH, Kim HS, Choi YJ, Kim N, Kim SJ. Prediction of pseudoprogression in patients with glioblastomas using the initial and final area under the curves ratio derived from dynamic contrast-enhanced T1-weighted perfusion MR imaging. AJNR Am J Neuroradiol 2013;34:2278-2286.
37. Elshafeey N, Kotrotsou A, Hassan A, et al. Multicenter study demonstrates radiomic features derived from magnetic resonance perfusion images identify pseudoprogression in glioblastoma. Nat Commun 2019;10:3170.
38. Park YW, Ahn SS, Moon JH, et al. Dynamic contrast-enhanced MRI may be helpful to predict response and prognosis after bevacizumab treatment in patients with recurrent high-grade glioma: comparison with diffusion tensor and dynamic susceptibility contrast imaging. Neuroradiology 2021;63:1811-1822.
39. Nguyen TB, Cron GO, Mercier JF, et al. Preoperative prognostic value of dynamic contrast-enhanced MRI-derived contrast transfer coefficient and plasma volume in patients with cerebral gliomas. AJNR Am J Neuroradiol 2015;36:63-69.
40. Choi YS, Kim DW, Lee SK, et al. The added prognostic value of preoperative dynamic contrast-enhanced MRI histogram analysis in patients with glioblastoma: analysis of overall and progression-free survival. AJNR Am J Neuroradiol 2015;36:2235-2241.
41. Kim HS, Kwon SL, Choi SH, et al. Prognostication of anaplastic astrocytoma patients: application of contrast leakage information of dynamic susceptibility contrast-enhanced MRI and dy-

namic contrast-enhanced MRI. Eur Radiol 2020;30:2171-2181.
42. Pak E, Choi KS, Choi SH, et al. Prediction of prognosis in glioblastoma using radiomics features of dynamic contrast-enhanced MRI. Korean J Radiol 2021;22:1514-1524.
43. Gouw AA, Seewann A, van der Flier WM, et al. Heterogeneity of small vessel disease: a systematic review of MRI and histopathology correlations. J Neurol Neurosurg Psychiatry 2011;82:126-135.
44. Park M, Moon Y, Han SH, Kim HK, Moon WJ. Myelin loss in white matter hyperintensities and normal-appearing white matter of cognitively impaired patients: a quantitative synthetic magnetic resonance imaging study. Eur Radiol 2019;29:4914-4921.
45. Li Y, Li M, Zhang X, et al. Higher blood-brain barrier permeability is associated with higher white matter hyperintensities burden. J Neurol 2017;264:1474-1481.
46. Wardlaw JM, Makin SJ, Hernández MCV, et al. Blood-brain barrier failure as a core mechanism in cerebral small vessel disease and dementia: evidence from a cohort study. Alzheimers Dement 2017;13:634-643.
47. Wong SM, Jansen JFA, Zhang CE, et al. Blood-brain barrier impairment and hypoperfusion are linked in cerebral small vessel disease. Neurology 2019;92:e1669-e1677.
48. Sweeney MD, Montagne A, Sagare AP, et al. Vascular dysfunction—The disregarded partner of Alzheimer's disease. Alzheimers Dement 2019;15:158-167.
49. Montagne A, Barnes SR, Sweeney MD, et al. Blood-brain barrier breakdown in the aging human hippocampus. Neuron 2015;85:296-302.
50. Nation DA, Sweeney MD, Montagne A, et al. Blood-brain barrier breakdown is an early biomarker of human cognitive dysfunction. Nat Med 2019;25:270-276.
51. van de Haar HJ, Burgmans S, Jansen JF, et al. Blood-brain barrier leakage in patients with early Alzheimer disease. Radiology 2016;281:527-535.
52. van de Haar HJ, Jansen JFA, van Osch MJP, et al. Neurovascular unit impairment in early Alzheimer's disease measured with magnetic resonance imaging. Neurobiol Aging 2016;45:190-196.
53. Montagne A, Nation DA, Sagare AP, et al. APOE4 leads to blood-brain barrier dysfunction predicting cognitive decline. Nature 2020;581:71-76.
54. Moon WJ, Lim C, Ha IH, et al. Hippocampal blood-brain barrier permeability is related to the APOE4 mutation status of elderly individuals without dementia. J Cereb Blood Flow Metab 2021;41:1351-1361.
55. Sweeney MD, Sagare AP, Zlokovic BV. Blood-brain barrier breakdown in Alzheimer disease and other neurodegenerative disorders. Nat Rev Neurol 2018;14:133-150.
56. Al-Bachari S, Naish JH, Parker GJM, Emsley HCA, Parkes LM. Blood–brain barrier leakage is increased in Parkinson's disease. Front Physiol 2020;11:593026.
57. Drouin-Ouellet J, Sawiak SJ, Cisbani G, et al. Cerebrovascular and blood-brain barrier impairments in Huntington's disease: potential implications for its pathophysiology. Ann Neurol 2015;78:160-177.
58. Cramer SP, Simonsen H, Frederiksen JL, Rostrup E, Larsson HB. Abnormal blood-brain barrier permeability in normal appearing white matter in multiple sclerosis investigated by MRI. Neuroimage Clin 2014;4:182-189.
59. Gaitán MI, Shea CD, Evangelou IE, et al. Evolution of the blood-brain barrier in newly forming multiple sclerosis lesions. Ann Neurol 2011;70:22-29.
60. Ingrisch M, Sourbron S, Morhard D, et al. Quantification of perfusion and permeability in multiple sclerosis: dynamic contrast-enhanced MRI in 3D at 3T. Invest Radiol 2012;47:252-258.
61. Villringer K, Sanz Cuesta BE, Ostwaldt AC, et al. DCE-MRI blood-brain barrier assessment in acute ischemic stroke. Neurology 2017;88:433-440.
62. Arba F, Rinaldi C, Caimano D, Vit F, Busto G, Fainardi E. Blood–brain barrier disruption and hemorrhagic transformation in acute ischemic stroke: systematic review and meta-analysis. Front Neurol 2020;11:594613.
63. Serlin Y, Ofer J, Ben-Arie G, et al. Blood-brain barrier leakage: a new biomarker in transient ischemic attacks. Stroke 2019;50:1266-1269.
64. Yoen H, Yoo RE, Choi SH, et al. Blood-brain barrier disruption in mild traumatic brain injury patients with post-concussion syndrome: evaluation with region-based quantification of dynamic contrast-enhanced MR imaging parameters using automatic whole-brain segmentation. Korean J Radiol 2021;22:118-130.
65. Kim YS, Kim M, Choi SH, et al. Altered vascular permeability in migraine-associated brain regions: evaluation with dynamic contrast-enhanced MRI. Radiology 2019;292:713-720.
66. Wu CH, Lirng JF, Wu HM, et al. Blood-brain barrier permeability in patients with reversible cerebral vasoconstriction syndrome assessed with dynamic contrast-enhanced MRI. Neurology 2021;97:e1847-e1859.
67. Raja R, Rosenberg GA, Caprihan A. MRI measurements of blood-brain barrier function in dementia: a review of recent studies. Neuropharmacology 2018;134(Pt B):259-271.
68. Cramer SP, Larsson HB. Accurate determination of blood-brain barrier permeability using dynamic contrast-enhanced T1-weighted MRI: a simulation and in vivo study on healthy subjects and multiple sclerosis patients. J Cereb Blood Flow Metab 2014;34:1655-1665.
69. Lim CM, Moon WJ. Methodologic concerns on the reported values for assessing permeability of the blood-brain barrier in the hippocampus. AJNR Am J Neuroradiol 2019;40:E65-E66.
70. Heye T, Davenport MS, Horvath JJ, et al. Reproducibility of dynamic contrast-enhanced MR imaging. Part I. Perfusion characteristics in the female pelvis by using multiple computer-aided diagnosis perfusion analysis solutions. Radiology 2013;266:801-811.
71. Rata M, Collins DJ, Darcy J, et al. Assessment of repeatability and treatment response in early phase clinical trials using DCE-MRI: comparison of parametric analysis using MR- and CT-derived arterial input functions. Eur Radiol 2016;26:1991-1998.
72. Filice S, Crisi G. Dynamic contrast-enhanced perfusion MRI of

high grade brain gliomas obtained with arterial or venous waveform input function. J Neuroimaging 2016;26:124-129.
73. Port RE, Knopp MV, Brix G. Dynamic contrast-enhanced MRI using Gd-DTPA: interindividual variability of the arterial input function and consequences for the assessment of kinetics in tumors. Magn Reson Med 2001;45:1030-1038.
74. Li X, Cai Y, Moloney B, et al. Relative sensitivities of DCE-MRI pharmacokinetic parameters to arterial input function (AIF) scaling. J Magn Reson 2016;269:104-112.
75. Huang W, Li X, Chen Y, et al. Variations of dynamic contrast-enhanced magnetic resonance imaging in evaluation of breast cancer therapy response: a multicenter data analysis challenge. Transl Oncol 2014;7:153-166.
76. Beuzit L, Eliat PA, Brun V, et al. Dynamic contrast-enhanced MRI: study of inter-software accuracy and reproducibility using simulated and clinical data. J Magn Reson Imaging 2016;43:1288-1300.